Hindawi Publishing Corporation
Journal of Spectroscopy
Volume 2015, Article ID 653848, 8 pages
http://dx.doi.org/10.1155/2015/653848

Research Article

Raman Spectroscopy Study of the Doping Effect of the Encapsulated Iron, Cobalt, and Nickel Bromides on Single-Walled Carbon Nanotubes

Marianna V. Kharlamova[1,2]

[1]*Department of Materials Science, Lomonosov Moscow State University, Leninskie Gory 1-3, Moscow 119991, Russia*
[2]*Faculty of Physics, University of Vienna, Strudlhofgasse 4, 1090 Vienna, Austria*

Correspondence should be addressed to Marianna V. Kharlamova; mv.kharlamova@gmail.com

Received 31 October 2014; Accepted 16 January 2015

Academic Editor: Shinichi Morita

In this contribution the modification of the electronic properties of single-walled carbon nanotubes (SWCNTs) filled with nickel bromide, cobalt bromide, and iron bromide was studied by Raman spectroscopy. The doping-induced alterations of the radial breathing mode (RBM) and G-mode in the Raman spectra of the filled SWCNTs were analyzed in detail. The observed shifts of the components of the Raman modes and changes of their profiles allowed concluding that the embedded compounds have an acceptor doping effect on the SWCNTs, and the doping level increases in the line with nickel bromide-cobalt bromide-iron bromide.

1. Introduction

The filling of single-walled carbon nanotubes (SWCNTs) is a promising approach for the modification of their electronic properties [1, 2]. In recent years, ways to fill SWCNTs with different types of substances were intensively explored. Metal halogenides ($RuCl_3$ [3], KI [4], LiI, NaI, RbI, CsI, AgI [5], CoI_2 [6], BaI_2 [7], PbI_2 [8], and MCl_3, where M = La, Nd, Sm, Eu, Gd, Tb, Yb [9]), metals (Au, Pt, Pd [10], Ag [10–12], Bi [13], Fe [14], and Ru [3]), and organic molecules ($(C_5H_5)_2Fe$ [15], $(C_5H_5)_2Co$, $(C_5H_5C_2H_5)_2Co$ [16], o-carborane [17], β-carotene [18], Zn(II), and Pt(II) porphyrin complexes [19]) were successfully encapsulated inside the SWCNT channels.

After these pioneer works, the electronic properties of filled nanotubes attracted further attention due to the large application potential of such nanostructures. It was demonstrated that metal halogenides ($CdCl_2$ [20, 21], $CdBr_2$, CdI_2 [20], $TbCl_3$, $ZnCl_2$ [21], $TmCl_3$ [22], $NiCl_2$, $NiBr_2$ [23], $CoBr_2$ [24], $FeCl_2$, $FeBr_2$, and FeI_2 [25]) cause acceptor doping of SWCNTs, whereas metals (Ag [26–28], Cu [28], Eu [29], and Er [30]) cause donor doping of nanotubes. At the same time, the chemical transformation of the encapsulated molecules ($(C_5H_5)_2Fe$ [31, 32], $(C_5H_5)_3Ce$ [33]) inside SWCNTs allows controlling the doping level and even switching between the doping types of SWCNTs. The possibility to precisely tailor the electronic properties of SWCNTs by filling their channels makes these nanohybrids promising for applications, for instance, in electronic device architectures [34, 35].

Raman spectroscopy is a very useful method for studying vibrational and electronic properties of carbon nanotubes [36, 37]. The investigation of the filled SWCNTs by this technique showed significant modifications of the Raman spectra of nanotubes upon their filling. The shifts of peaks of the radial breathing mode (RBM) and G-mode as well as changes in their profiles were assigned to the alteration of the electronic structure of SWCNTs as a result of doping and hybridization effects. For SWCNTs filled with electron acceptors ($TmCl_3$ [22], $TbCl_3$, $ZnCl_2$ [21], $NiCl_2$, $NiBr_2$ [23], $CoBr_2$ [24], $CdCl_2$ [20, 21], $CdBr_2$, CdI_2 [20], $FeCl_2$, $FeBr_2$, and FeI_2 [25]) changes in the relative intensities of the RBM peaks were observed, which were attributed to the doping-induced shift of the resonance excitation energy of nanotubes. Also, the significant upshifts of the G-band peaks were reported, which were accompanied by the change of

the band profile to semiconducting type. For SWCNTs filled with electron donors (Ag [26–28], Cu [28]) the shifts of the RBM and G-band peaks were observed, and they were typically accompanied by the switching of the G-band shape to metallic type.

In most reports only a qualitative description of the Raman spectra of the filled SWCNTs was performed. However, a detailed investigation of the spectra with a quantitative analysis of the relative intensities of the individual peaks in the RBM and G-bands opens a way to studying precisely the correlation between the type of the encapsulated compound and its influence on the electronic properties of SWCNTs, as well as the dependence of the Raman modes on the doping level.

In the present work a detailed Raman spectroscopy study of the doping effect of encapsulated nickel bromide ($NiBr_2$) [23], cobalt bromide ($CoBr_2$) [24], and iron bromide ($FeBr_2$) [25] on SWCNTs was performed. The doping-induced alterations of the radial breathing mode (RBM) and G-mode in the Raman spectra of the filled SWCNTs were analyzed. The data showed that the incorporated metal bromides have an acceptor doping effect on the nanotubes; however, the doping level depends on the compound. The inserted nickel bromide causes the smallest doping of SWCNTs, whereas iron bromide causes the largest.

2. Materials and Methods

SWCNTs with a mean diameter of 1.4 nm synthesized by the catalytic arc-discharge method were used as a starting material. The synthesis was conducted using 0.8 cm-diameter graphite rods with Y/Ni catalyst at 73.3 kPa helium pressure and a current of 100–110 A [38]. The synthesized SWCNTs were purified by repeated oxygenation at 350–450°C in air and rinsing with hydrochloric acid (HCl). The purified samples had a SWCNT content of 78 wt.% and a catalyst content of 0.12 wt.%.

Before the filling procedure, the SWCNTs were annealed at 500°C in dry air for 30 minutes, in order to open their ends. The obtained nanotube sample ($m = 0.025$ g) was grinded with anhydrous $NiBr_2$, $CoBr_2$, or $FeBr_2$ (Aldrich, 99.999 wt.%) in a molar ratio of 1 : 1 in a glove box, in order to prevent hydration of the salts. The mixture was evacuated in a quartz ampoule to a pressure below 10^{-5} Torr for 2 hours and sealed. The ampoule was heated at a rate of 1°C/min to the temperature of 1063°C (for $NiBr_2$), 778°C (for $CoBr_2$), or 784°C (for $FeBr_2$). This temperature was kept for 10 hours, after that the samples were slowly cooled down at a rate of 0.02–1°C/min [23–25]. The obtained samples are labeled $NiBr_2$@SWCNT, $CoBr_2$@SWCNT, and $FeBr_2$@SWCNT.

The Raman spectra were acquired using a Renishaw InVia Raman microscope equipped with 17 mW 633 nm ($E_{ex} = 1.96$ eV) HeNe and 300 mW 785 nm ($E_{ex} = 1.58$ eV) near-infrared diode lasers, variable power neutral density filters (power range 0.00005–100%), and near-excitation tunable filters. The samples were prepared by dispersing the filled nanotubes in hexane with subsequent dropping this dispersion onto silicon wafers. The Raman spectra were fitted by the Lorentzian, Voigt, and Fano peaks with the PeakFit v4.12 program.

3. Results and Discussion

Using lasers with two energies 1.58 eV and 1.96 eV allowed exciting electronic transitions between van Hove singularities (vHs) of metallic and semiconducting SWCNTs of different diameters. As follows from the Kataura plot, the laser with an energy of 1.58 eV initiates the electronic transitions between the first vHs of metallic SWCNTs (E_{11}^M) with a diameter of 1.4–1.5 nm. The laser with an energy of 1.96 eV excites the electronic transitions between the first vHs of metallic nanotubes with a diameter of 1.4 nm and between the third vHs of semiconducting SWCNTs with a diameter of ~1.6 nm (E_{33}^S) [39].

Figure 1 demonstrates the Raman spectra of the pristine SWCNTs, $NiBr_2$@SWCNT, $CoBr_2$@SWCNT, and $FeBr_2$@SWCNT samples acquired at laser energies of 1.58 eV and 1.96 eV. Here two main regions of the Raman spectra are shown: a radial breathing mode (RBM), which corresponds to synchronous radial vibrations of carbon atoms (A_{1g} symmetry), and a G-band, which belongs to C–C bond vibrations (A, E_1, and E_2 symmetries [36]) [40]. The RBM band of the Raman spectrum of the pristine SWCNTs acquired at 1.58 eV contains two peaks at 157 and 171 cm^{-1} (Figure 1(a)), which are assigned to 1.5- and 1.4-nm metallic nanotubes, accordingly [41]. The G-band of the spectrum includes three peaks at 1556, 1571, and 1593 cm^{-1}. The component at 1556 cm^{-1} belongs to the G^--mode, which originates from the longitudinal optical (LO) phonon in metallic SWCNTs. Two components at higher frequencies correspond to the G^+-mode of semiconducting SWCNTs. The first component at 1571 cm^{-1} (G^+_{TO}) belongs to the transversal optical (TO) phonon, and the second component at 1593 cm^{-1} (G^+_{LO}) belongs to the longitudinal optical phonon [42, 43]. The G-band has a broad asymmetric shape, which is typical of metallic SWCNTs [40, 44]. The RBM-band of the Raman spectrum of the pristine nanotubes acquired at 1.96 eV contains two peaks at 151 and 169 cm^{-1} (Figure 1(b)), which can be assigned to ~1.5-nm semiconducting SWCNTs and 1.4-nm metallic nanotubes, respectively [41]. The G-band of the spectrum includes three components at 1546, 1565, and 1591 cm^{-1} (G^-, G^+_{TO}, and G^+_{LO}, resp.) and has a metallic profile.

The Raman spectra of the $NiBr_2$-, $CoBr_2$-, and $FeBr_2$-filled nanotubes acquired at laser energies of 1.58 eV and 1.96 eV show significant differences in comparison with the corresponding spectra of the pristine SWCNTs. The peaks in the RBM-band of the filled SWCNTs are upshifted by up to 14 cm^{-1}, and the RBM-band also alters the profile (Figure 1). This is possibly connected with changes in the resonance excitation conditions of the SWCNTs upon their filling. The peaks in the G-band of the filled SWCNTs are significantly shifted towards higher frequencies by up to 15 cm^{-1}. Additionally, the G-band modifies the profile from a broad asymmetric Breit-Wigner-Fano shape of metallic SWCNTs to a narrow Lorentzian shape of semiconducting

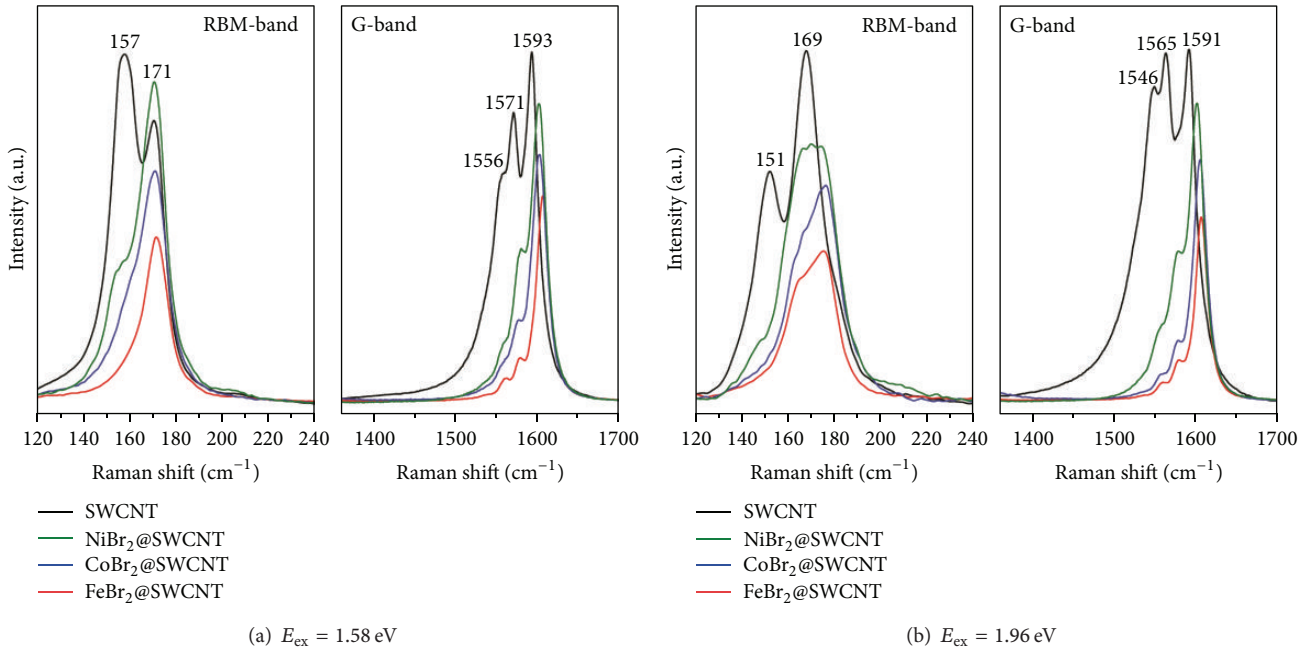

FIGURE 1: The RBM- and G-bands of the Raman spectra of the pristine SWCNTs, $NiBr_2$@SWCNT, $CoBr_2$@SWCNT, and $FeBr_2$@SWCNT samples acquired at laser energies of 1.58 eV (a) and 1.96 eV (b).

nanotubes [40, 44]. These changes are probably caused by the modification of the electronic structure of the filled SWCNTs due to a charge transfer from the nanotube walls to the encapsulated salts, that is, acceptor doping of nanotubes [23–25].

The RBM and G-bands of the Raman spectra of the $NiBr_2$-, $CoBr_2$-, and $FeBr_2$-filled nanotubes demonstrate similar trends of shifts of the peaks and changes in the band profiles. However, the shift values and degrees of the profile change depend on the metal bromide. These changes are also dependent on the laser energy, at which the Raman spectra were acquired.

The detailed analysis of the Raman spectra of the pristine and metal bromide-filled SWCNTs acquired at a laser energy of 1.58 eV is shown in Figure 2. The RBM-bands of the Raman spectra are fitted with two components (C 1 and C 2), corresponding to SWCNTs of different diameters. The G-bands are fitted with one component of metallic SWCNTs (G^-) and two components of semiconducting nanotubes (G^+_{TO} and G^+_{LO}), which were discussed above. Table 1 summarizes the peak positions and calculated relative integral intensities of the individual components. The RBM-band of the Raman spectrum of the $NiBr_2$-filled SWCNTs does not show shifts of the components as compared to the spectrum of the pristine nanotubes (Figure 2(a)). However, their relative intensities change. The relative intensity of the component C 2 increases from 0.41 to 0.75, and the peak of 1.4 nm-metallic SWCNTs has the maximal intensity (Figure 2(b)). This fact implies the change in the resonance excitation energy of 1.5-nm metallic SWCNTs. As a result, the laser with an energy of 1.58 eV excites smaller diameter nanotubes. The RBM-bands of the spectra of the $CoBr_2$- and $FeBr_2$-filled SWCNTs show a small upshift of the components by 1–3 cm^{-1} (Figures 2(c) and 2(d)). Also, there is a larger increase in the relative intensity of the component C 2 to 0.77 for $CoBr_2$@SWCNT and to 0.87 for $FeBr_2$@SWCNT (Table 1).

The G-band of the Raman spectra of the metal bromide-filled SWCNTs demonstrates upshifts of the components that increase from $NiBr_2$@SWCNT to $CoBr_2$@SWCNT to $FeBr_2$@SWCNT. The upshift of the G^--component increases from 1 to 2 to 4 cm^{-1}, the upshift of the G^+_{TO}-component increases from 5 to 6 to 7 cm^{-1}, and the upshift of the G^+_{LO}-component increases from 8 to 9 to 13 cm^{-1} in this line (Table 1). Moreover, the Raman spectra of the filled SWCNTs show the change in the G-band profile, which is a consequence of the change of the relative intensities of the individual components (Figure 2). In particular, there is a significant decrease in the relative intensity of the component of metallic SWCNTs (G^-). It drops from 0.44 for the pristine SWCNTs to 0.09 for $NiBr_2$@SWCNT, 0.08 for $CoBr_2$@SWCNT, and 0.05 for $FeBr_2$@SWCNT (Table 1).

Figure 3 illustrates the changes observed in the RBM- and G-bands of the Raman spectra of the metal bromide-filled SWCNTs acquired at a laser energy of 1.58 eV in comparison with the spectrum of the pristine nanotubes. The observed alteration of the relative intensities of the RBM components and their shifts are caused by changes in the resonance excitation conditions of SWCNTs upon their filling. The modifications of the RBM band become larger in line with $NiBr_2$-$CoBr_2$-$FeBr_2$ (Figure 3(a)). The G-band of the Raman spectrum of the iron bromide-filled SWCNTs also shows the largest shifts of the components and the most significant decrease in the relative intensity of the metallic component, whereas the spectrum of the nickel

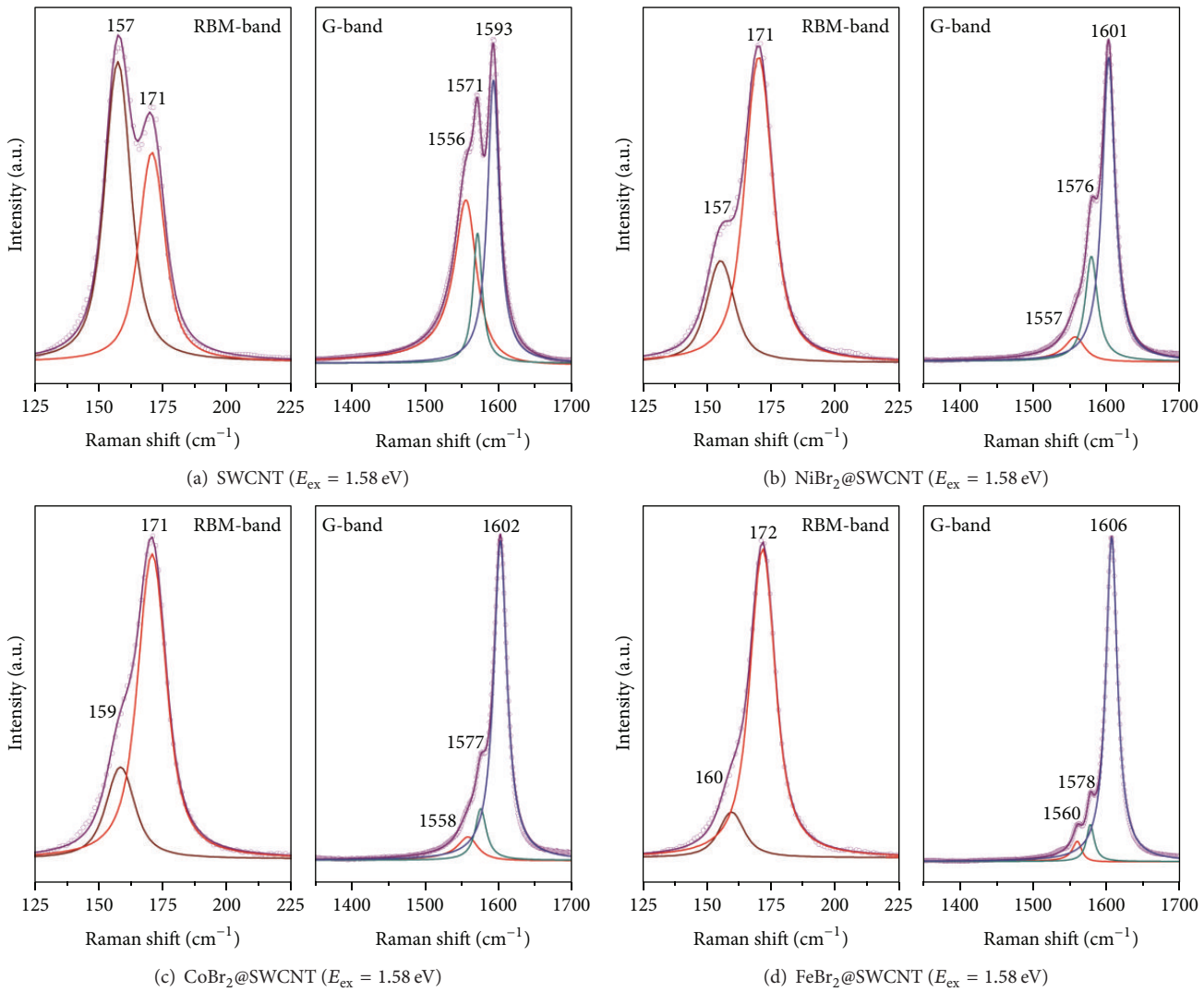

FIGURE 2: The fitting of the RBM- and G-bands of the Raman spectra of the pristine SWCNTs (a), $NiBr_2$@SWCNT (b), $CoBr_2$@SWCNT (c), and $FeBr_2$@SWCNT (d) samples acquired at a laser energy of 1.58 eV. The RBM-bands include two components, which belong to the nanotubes of different diameters. The G-bands include one component of metallic SWCNTs (G^- at the lowest frequencies) and two components of semiconducting SWCNTs (G^+_{TO} at lower and G^+_{LO} at higher frequencies).

bromide-filled SWCNTs demonstrates the smallest changes (Figure 3(b)). This indicates the strongest acceptor doping of SWCNTs by the encapsulated $FeBr_2$ and the weakest doping of SWCNTs by the introduced $NiBr_2$.

Figure 4 demonstrates the fitting of the RBM- and G-bands of the Raman spectra of the pristine and metal bromide-filled SWCNTs acquired at a laser energy of 1.96 eV with individual components. The RBM-bands of the Raman spectra of the filled SWCNTs show a significant shift of the components by up to 14 cm^{-1} for C 1 and 8 cm^{-1} for C 2, which is much larger than in the spectra acquired at a laser energy of 1.58 eV, discussed above. There is also the alteration of the relative intensities of the RBM components. In all spectra the relative intensity of the component C 2 decreases as compared to the pristine nanotubes. The value changes from 0.66 for SWCNTs to 0.54 for $NiBr_2$@SWCNT, 0.65 for $CoBr_2$@SWCNT, and 0.60 for $FeBr_2$@SWCNT (Table 1), which corresponds to a slight change in the resonance excitation conditions for the filled nanotubes. However, no dependence of the modifications of the RBM band on the compound is observed.

The G-band of the metal bromide-filled SWCNTs demonstrates upshifts of the components that are larger than those observed in the Raman spectra acquired at a laser energy of 1.58 eV. They increase from $NiBr_2$@SWCNT to $CoBr_2$@SWCNT to $FeBr_2$@SWCNT (Figure 4). The upshift of the G^--component increases from 8 to 10 to 12 cm^{-1}, the upshift of the G^+_{TO}-component increases from 10 to 11 to 13 cm^{-1}, and the upshift of the G^+_{LO}-component increases from 11 to 13 to 15 cm^{-1} in this line (Table 1). As for the case of the 1.58 eV-energy laser, the Raman spectra of the filled SWCNTs show the alteration of the G-band profile due to the significant decrease of the relative intensity of the component of metallic SWCNTs (G^-). It decreases from 0.47 for

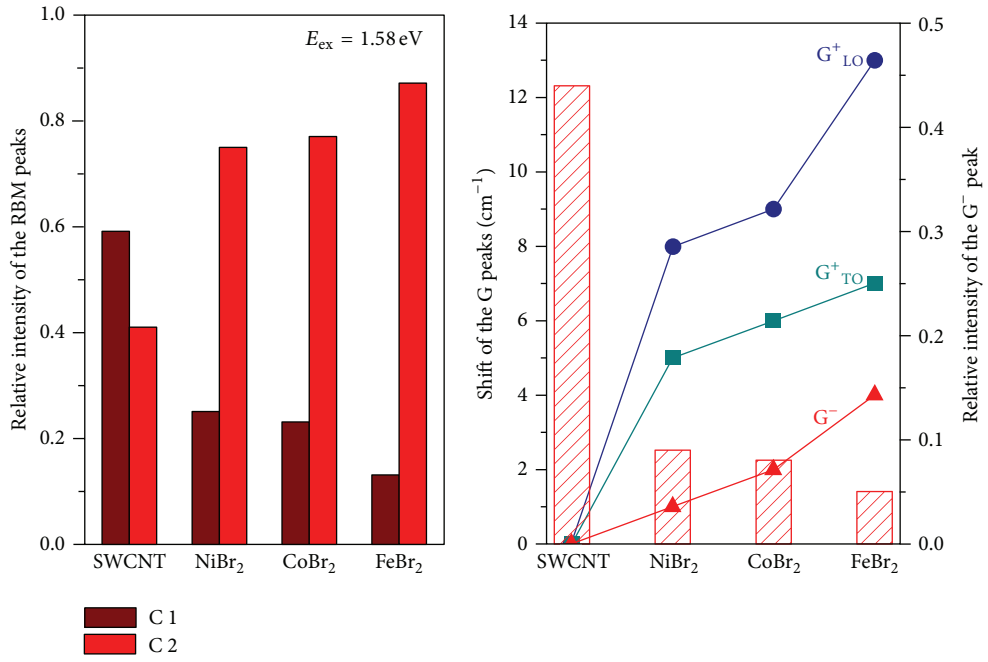

(a) RBM-band X@SWCNT (b) G-band X@SWCNT

Figure 3: The relative intensity of the RBM components (C 1 and C 2) (a), the shift of the G-band components (G^-, G^+_{TO} and G^+_{LO}), and the relative intensity of the G^--component (b) in the Raman spectra of the pristine SWCNTs, $NiBr_2$@SWCNT, $CoBr_2$@SWCNT, and $FeBr_2$@SWCNT samples, acquired at a laser energy of 1.58 eV.

Table 1: The positions (RS) and relative intensities (I) of the components of the RBM-bands (C 1 and C 2) and G-bands (metallic G^- and semiconducting G^+_{TO} and G^+_{LO}) of the Raman spectra of the pristine SWCNTs, $NiBr_2$@SWCNT, $CoBr_2$@SWCNT, and $FeBr_2$@SWCNT samples, acquired at laser energies of 1.58 eV and 1.96 eV. In the parentheses the shifts of the component positions in comparison to ones of the pristine SWCNTs are given. The experimental error in the component positions equals ±0.5 cm^{-1}.

Sample	RBM-band, cm^{-1}				G-band, cm^{-1}					
	C 1		C 2		G^-		G^+_{TO}		G^+_{LO}	
	RS	I	RS	I	RS	I	RS	I	RS	I
E_{ex} = 1.58 eV										
SWCNT	157	0.59	171	0.41	1556	0.44	1571	0.15	1593	0.41
$NiBr_2$@SWCNT	157	0.25	171	0.75	1557 (+1)	0.09	1576 (+5)	0.23	1601 (+8)	0.68
$CoBr_2$@SWCNT	159 (+2)	0.23	171	0.77	1558 (+2)	0.08	1577 (+6)	0.11	1602 (+9)	0.81
$FeBr_2$@SWCNT	160 (+3)	0.13	172 (+1)	0.87	1560 (+4)	0.05	1578 (+7)	0.07	1606 (+13)	0.88
E_{ex} = 1.96 eV										
SWCNT	151	0.34	169	0.66	1546	0.47	1565	0.16	1591	0.37
$NiBr_2$@SWCNT	164 (+13)	0.46	175 (+6)	0.54	1554 (+8)	0.12	1575 (+10)	0.27	1602 (+11)	0.61
$CoBr_2$@SWCNT	165 (+14)	0.35	177 (+8)	0.65	1556 (+10)	0.05	1576 (+11)	0.10	1604 (+13)	0.85
$FeBr_2$@SWCNT	164 (+13)	0.40	176 (+7)	0.60	1558 (+12)	0.04	1578 (+13)	0.10	1606 (+15)	0.86

the SWCNTs to 0.12 for the $NiBr_2$-filled SWCNTs, 0.05 for the $CoBr_2$-filled SWCNTs, and 0.04 for the $FeBr_2$-filled SWCNTs (Table 1).

Figure 5 summarizes the modifications observed in the Raman spectra of the filled SWCNTs acquired at a laser energy of 1.96 eV. Although the changes in the RBM-bands do not show a clear dependence on the compound, the shifts and alterations of the intensities of the components of the G-bands increase in line with nickel bromide-cobalt bromide-iron bromide. This implies that the encapsulated $FeBr_2$ causes the largest acceptor doping level of SWCNTs, whereas $NiBr_2$ causes the smallest. This conclusion is in agreement with the results obtained at a laser energy of 1.58 eV.

The doping of SWCNTs by the introduced metal bromides is a result of a large difference in the work functions of the compounds and nanotubes. It leads to the charge transfer from the SWCNTs to the inserted salts, accompanied

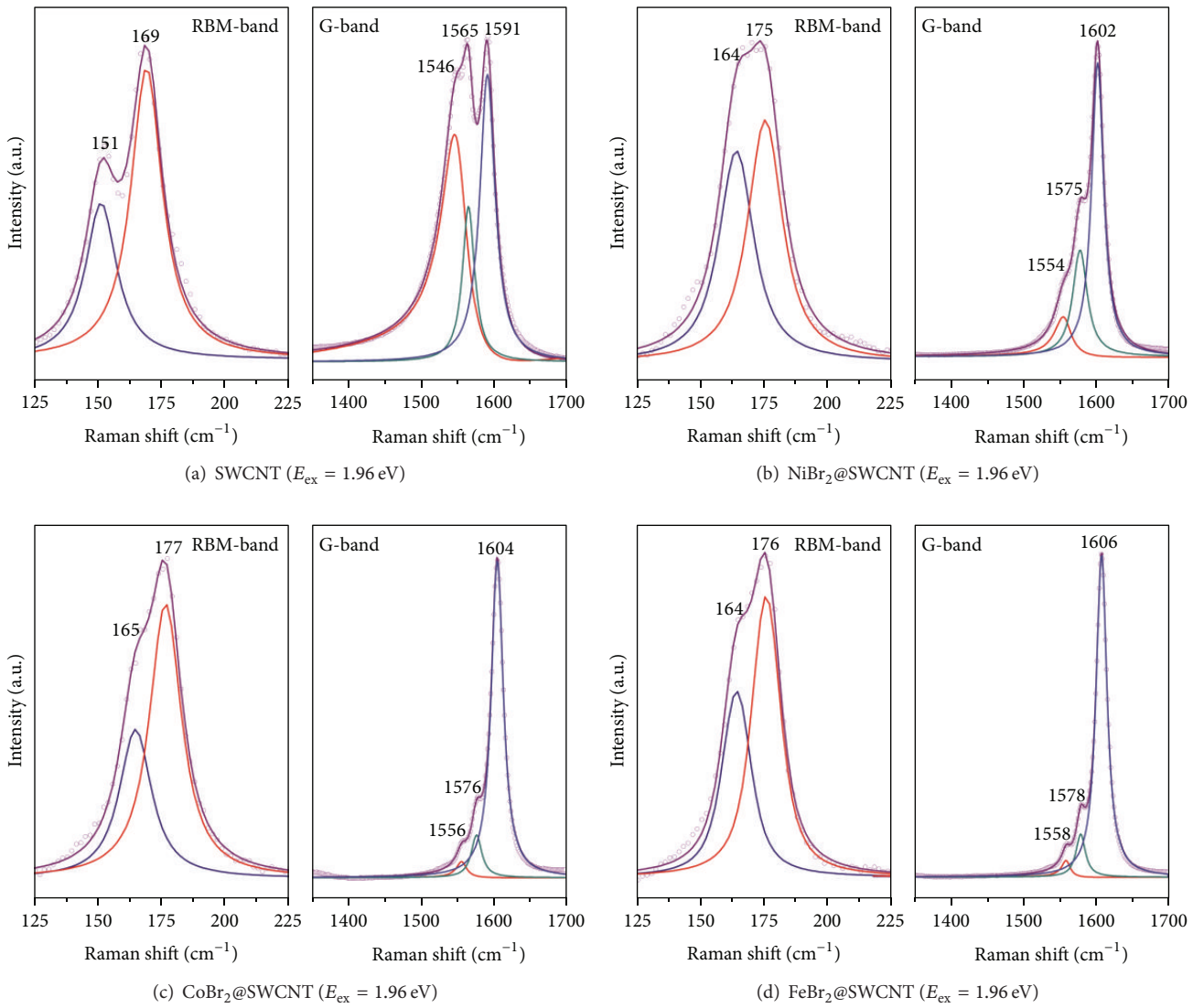

(a) SWCNT (E_{ex} = 1.96 eV)

(b) $NiBr_2$@SWCNT (E_{ex} = 1.96 eV)

(c) $CoBr_2$@SWCNT (E_{ex} = 1.96 eV)

(d) $FeBr_2$@SWCNT (E_{ex} = 1.96 eV)

Figure 4: The fitting of the RBM- and G-bands of the Raman spectra of the pristine SWCNTs (a), $NiBr_2$@SWCNT (b), $CoBr_2$@SWCNT (c), and $FeBr_2$@SWCNT (d) samples acquired at a laser energy of 1.96 eV. The RBM-bands include two components, which belong to the nanotubes of different diameters. The G-bands include one component of metallic SWCNTs (G^- at the lowest frequencies) and two components of semiconducting SWCNTs (G^+_{TO} at lower and G^+_{LO} at higher frequencies).

by equalizing their Fermi levels. The observed differences in the doping levels for the $NiBr_2$, $CoBr_2$, and $FeBr_2$-filled nanotubes are probably caused by their different chemical properties. These compounds differ only by the metal cation and, therefore, the metal type influences the doping effect on nanotubes. Indeed, the chemical properties (e.g., atomic and cation radii, electron affinity) of transition metals evenly change from nickel to cobalt to iron, and this fact may explain the observed tendency in the increase of the acceptor doping effect of SWCNTs from the incorporated $NiBr_2$ to $CoBr_2$ to $FeBr_2$.

4. Conclusions

In conclusion, in this contribution the doping effect of the encapsulated nickel bromide, cobalt bromide, and iron bromide on the SWCNTs was compared on the basis of the Raman spectroscopy data. The conducted detailed analysis of the Raman spectra of the pristine and filled SWCNTs allowed precise investigation of the doping-induced modifications of the Raman modes. The observed shifts of the components of the RBM and G-bands of the Raman spectra and alteration of the band profiles allowed concluding that the incorporated metal bromides have acceptor doping effect on the SWCNTs, and the doping efficiency increases in the line with nickel bromide-cobalt bromide-iron bromide.

Conflict of Interests

The author declares that there is no conflict of interests regarding the publication of this paper.

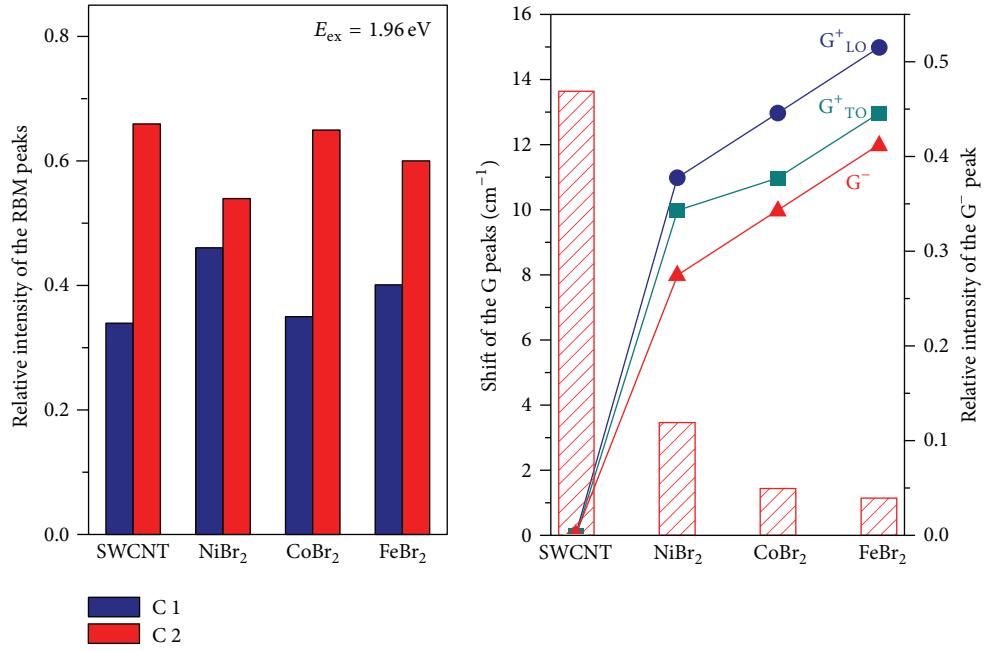

(a) RBM-band X@SWCNT

(b) G-band X@SWCNT

FIGURE 5: The relative intensity of the RBM components (C 1 and C 2) (a), the shift of the G-band components (G^-, G^+_{TO}, and G^+_{LO}) and the relative intensity of the G^--component (b) in the Raman spectra of the pristine SWCNTs, $NiBr_2$@SWCNT, $CoBr_2$@SWCNT, and $FeBr_2$@SWCNT samples, acquired at a laser energy of 1.96 eV.

Acknowledgment

The author acknowledges the Austrian Academy of Sciences for a DOC-fFORTE fellowship.

References

[1] M. Monthioux, E. Flahaut, and J. P. Cleuziou, "Hybrid carbon nanotubes: Strategy, progress and perspectives," *Journal of Materials Research*, vol. 21, no. 11, pp. 2774–2793, 2006.

[2] M. V. Kharlamova, "Electronic properties of pristine and modified single-walled carbon nanotubes," *Physics—Uspekhi*, vol. 56, no. 11, pp. 1047–1073, 2013.

[3] J. Sloan, J. Hammer, M. Zwiefka-Sibley, and M. L. H. Green, "The opening and filling of single walled carbon nanotubes (SWTs)," *Chemical Communications*, no. 3, pp. 347–348, 1998.

[4] R. R. Meyer, J. Sloan, R. E. Dunin-Borkowski et al., "Discrete atom imaging of one-dimensional crystals formed within single-walled carbon nanotubes," *Science*, vol. 289, no. 5483, pp. 1324–1326, 2000.

[5] J. Sloan, A. I. Kirkland, J. L. Hutchison, and M. L. H. Green, "Aspects of crystal growth within carbon nanotubes," *Comptes Rendus Physique*, vol. 4, no. 9, pp. 1063–1074, 2003.

[6] E. Philp, J. Sloan, A. I. Kirkland et al., "An encapsulated helical one-dimensional cobalt iodide nanostructure," *Nature Materials*, vol. 2, no. 12, pp. 788–791, 2003.

[7] J. Sloan, S. J. Grosvenor, S. Friedrichs, A. I. Kirkland, J. L. Hutchison, and M. L. H. Green, "One-dimensional BaI2chain with five- and six-coordination, formed within a single-walled carbon nanotube," *Angewandte Chemie International Edition*, vol. 41, no. 7, pp. 1156–1159, 2002.

[8] E. Flahaut, J. Sloan, S. Friedrichs et al., "Crystallization of 2H and 4H PbI_2 in carbon nanotubes of varying diameters and morphologies," *Chemistry of Materials*, vol. 18, no. 8, pp. 2059–2069, 2006.

[9] C. G. Xu, J. Sloan, G. Brown et al., "1D lanthanide halide crystals inserted into single-walled carbon nanotubes," *Chemical Communications*, vol. 24, pp. 2427–2428, 2000.

[10] A. Govindaraj, B. C. Satishkumar, M. Nath, and C. N. R. Rao, "Metal nanowires and intercalated metal layers in single-walled carbon nanotube bundles," *Chemistry of Materials*, vol. 12, no. 1, pp. 202–205, 2000.

[11] J. Sloan, D. M. Wright, H.-G. Woo et al., "Capillarity and silver nanowire formation observed in single walled carbon nanotubes," *Chemical Communications*, no. 8, pp. 699–700, 1999.

[12] Z. L. Zhang, B. Li, Z. J. Shi, Z. N. Gu, Z. Q. Xue, and L.-M. Peng, "Filling of single-walled carbon nanotubes with silver," *Journal of Materials Research*, vol. 15, no. 12, pp. 2658–2661, 2000.

[13] C.-H. Kiang, J.-S. Choi, T. T. Tran, and A. D. Bacher, "Molecular nanowires of 1 nm diameter from capillary filling of single-walled carbon nanotubes," *Journal of Physical Chemistry B*, vol. 103, no. 35, pp. 7449–7451, 1999.

[14] E. Borowiak-Palen, E. Mendoza, A. Bachmatiuk et al., "Iron filled single-wall carbon nanotubes—a novel ferromagnetic medium," *Chemical Physics Letters*, vol. 421, no. 1–3, pp. 129–133, 2006.

[15] L. H. Guan, Z. J. Shi, M. X. Li, and Z. N. Gu, "Ferrocene-filled single-walled carbon nanotubes," *Carbon*, vol. 43, no. 13, pp. 2780–2785, 2005.

[16] L.-J. Li, A. N. Khlobystov, J. G. Wiltshire, G. A. D. Briggs, and R. J. Nicholas, "Diameter-selective encapsulation of metallocenes

in single-walled carbon nanotubes," *Nature Materials*, vol. 4, no. 6, pp. 481–485, 2005.

[17] D. A. Morgan, J. Sloan, and M. L. H. Green, "Direct imaging of o-carborane molecules within single walled carbon nanotubes," *Chemical Communications*, no. 20, pp. 2442–2443, 2002.

[18] K. Yanagi, Y. Miyata, and H. Kataura, "Highly stabilized β-carotene in carbon nanotubes," *Advanced Materials*, vol. 18, no. 4, pp. 437–441, 2006.

[19] H. Kataura, Y. Maniwa, M. Abe et al., "Optical properties of fullerene and non-fullerene peapods," *Applied Physics A: Materials Science and Processing*, vol. 74, no. 3, pp. 349–354, 2002.

[20] M. V. Kharlamova, L. V. Yashina, and A. V. Lukashin, "Charge transfer in single-walled carbon nanotubes filled with cadmium halogenides," *Journal of Materials Science*, vol. 48, no. 24, pp. 8412–8419, 2013.

[21] M. V. Kharlamova, "Comparison of influence of incorporated 3d-, 4d- and 4f-metal chlorides on electronic properties of single-walled carbon nanotubes," *Applied Physics A: Materials Science and Processing*, vol. 111, no. 3, pp. 725–731, 2013.

[22] M. V. Kharlamova, L. V. Yashina, and A. V. Lukashin, "Comparison of modification of electronic properties of single-walled carbon nanotubes filled with metal halogenide, chalcogenide, and pure metal," *Applied Physics A: Materials Science and Processing*, vol. 112, no. 2, pp. 297–304, 2013.

[23] M. V. Kharlamova, L. V. Yashina, A. A. Eliseev et al., "Single-walled carbon nanotubes filled with nickel halogenides: atomic structure and doping effect," *Physica Status Solidi B*, vol. 249, no. 12, pp. 2328–2332, 2012.

[24] M. V. Kharlamova, A. A. Eliseev, L. V. Yashina et al., "Study of the electronic structure of single-walled carbon nanotubes filled with cobalt bromide," *JETP Letters*, vol. 91, no. 4, pp. 196–200, 2010.

[25] M. V. Kharlamova, M. M. Brzhezinskay, A. S. Vinogradov et al., "The formation and properties of one-dimensional $FeHal_2$ (Hal = Cl, Br, I) nanocrystals in channels of single-walled carbon nanotubes," *Nanotechnologies in Russia*, vol. 4, no. 9-10, pp. 634–646, 2009.

[26] P. Corio, A. P. Santos, P. S. Santos et al., "Characterization of single wall carbon nanotubes filled with silver and with chromium compounds," *Chemical Physics Letters*, vol. 383, no. 5-6, pp. 475–480, 2004.

[27] E. Borowiak-Palen, M. H. Ruemmeli, T. Gemming, T. Pichler, R. J. Kalenczuk, and S. R. P. Silva, "Silver filled single-wall carbon nanotubes—synthesis, structural and electronic properties," *Nanotechnology*, vol. 17, no. 9, pp. 2415–2419, 2006.

[28] M. V. Kharlamova and J. J. Niu, "Comparison of metallic silver and copper doping effects on single-walled carbon nanotubes," *Applied Physics A*, vol. 109, no. 1, pp. 25–29, 2012.

[29] R. Nakanishi, R. Kitaura, P. Ayala et al., "Electronic structure of Eu atomic wires encapsulated inside single-wall carbon nanotubes," *Physical Review B—Condensed Matter and Materials Physics*, vol. 86, no. 11, Article ID 115445, 2012.

[30] P. Ayala, R. Kitaura, R. Nakanishi et al., "Templating rare-earth hybridization via ultrahigh vacuum annealing of $ErCl_3$ nanowires inside carbon nanotubes," *Physical Review B—Condensed Matter and Materials Physics*, vol. 83, no. 8, 6 pages, 2011.

[31] H. Shiozawa, T. Pichler, C. Kramberger et al., "Fine tuning the charge transfer in carbon nanotubes via the interconversion of encapsulated molecules," *Physical Review B—Condensed Matter and Materials Physics*, vol. 77, no. 15, Article ID 153402, 2008.

[32] H. Shiozawa, T. Pichler, A. Grüneis et al., "A catalytic reaction inside a single-walled carbon nanotube," *Advanced Materials*, vol. 20, no. 8, pp. 1443–1449, 2008.

[33] H. Shiozawa, T. Pichler, C. Kramberger et al., "Screening the missing electron: nanochemistry in action," *Physical Review Letters*, vol. 102, no. 4, Article ID 046804, 2009.

[34] P. M. Ajayan and O. Z. Zhou, *Carbon Nanotubes*, vol. 80 of *Topics in Applied Physics*, Springer, Heidelberg, Germany, 2001, M. Dresselhaus, G. Dresselhaus, and P. Avouris, Eds.

[35] M. Endo, M. S. Strano, and P. M. Ajayan, "Potential applications of carbon nanotubes," in *Carbon Nanotubes*, A. Jorio, G. Dresselhaus, and M. Dresselhaus, Eds., vol. 111 of *Topics in Applied Physics*, pp. 13–62, Springer, Heidelberg, Germany, 2008.

[36] M. S. Dresselhaus and P. C. Eklund, "Phonons in carbon nanotubes," *Advances in Physics*, vol. 49, no. 6, pp. 705–814, 2000.

[37] M. S. Dresselhaus, G. Dresselhaus, R. Saito, and A. Jorio, "Raman spectroscopy of carbon nanotubes," *Physics Reports*, vol. 409, no. 2, pp. 47–99, 2005.

[38] A. V. Krestinin, M. B. Kislov, and A. G. Ryabenko, "Formation of nanofibers and nanotubes production," in *Mathematics, Physics and Chemistry*, S. Gucery, Y. G. Gogotsi, and V. Kuznetsov, Eds., vol. 169 of *NATO Science Series II*, Kluwer Academic, Dordrecht, The Netherlands, 2004.

[39] H. Kataura, Y. Kumazawa, Y. Maniwa et al., "Optical properties of single-wall carbon nanotubes," *Synthetic Metals*, vol. 103, no. 1–3, pp. 2555–2558, 1999.

[40] M. S. Dresselhaus, G. Dresselhaus, A. Jorio, A. G. S. Filho, and R. Saito, "Raman spectroscopy on isolated single wall carbon nanotubes," *Carbon*, vol. 40, no. 12, pp. 2043–2061, 2002.

[41] P. T. Araujo, I. O. Maciel, P. B. C. Pesce et al., "Nature of the constant factor in the relation between radial breathing mode frequency and tube diameter for single-wall carbon nanotubes," *Physical Review B—Condensed Matter and Materials Physics*, vol. 77, no. 24, Article ID 241403, 2008.

[42] A. Jorio, M. A. Pimenta, A. G. S. Filho, R. Saito, G. Dresselhaus, and M. S. Dresselhaus, "Characterizing carbon nanotube samples with resonance Raman scattering," *New Journal of Physics*, vol. 5, article 139, 2003.

[43] M. Fouquet, H. Telg, J. Maultzsch et al., "Longitudinal optical phonons in metallic and semiconducting carbon nanotubes," *Physical Review Letters*, vol. 102, no. 7, Article ID 075501, 2009.

[44] S. D. M. Brown, P. Corio, A. Marucci, M. S. Dresselhaus, M. A. Pimenta, and K. Kneipp, "Anti-Stokes Raman spectra of single-walled carbon nanotubes," *Physical Review B*, vol. 61, no. 8, pp. R5137–R5140, 2000.